Geophys. J. Int. (2000) **142,** 151–161

A damage mechanics model for power-law creep and earthquake aftershock and foreshock sequences

Ian G. Main

Department of Geology & Geophysics, University of Edinburgh, West Mains Road, Edinburgh EH9 3JW, *UK. E-mail: ian.main@ed.ac.uk*

Accepted 2000 February 18. Received 1999 December 23; in original form 1999 September 22

SUMMARY

It is common practice to refer to three independent stages of creep under static loading conditions in the laboratory: namely transient, steady-state, and accelerating. Here we suggest a simple damage mechanics model for the apparently trimodal behaviour of the strain and event rate dependence, by invoking two local mechanisms of positive and negative feedback applied to constitutive rules for time-dependent subcritical crack growth. In both phases, the individual constitutive rule for measured strain ε takes the form $\varepsilon(t) = \varepsilon_0[1 + t/m\tau]^m$, where τ is the ratio of initial crack length to rupture velocity. For a local hardening mechanism (negative feedback), we find that transient creep dominates, with $0 < m < 1$. Crack growth in this stage is stable and decelerating. For a local softening mechanism (positive feedback), $m < 0$, and crack growth is unstable and accelerating. In this case a quasi-static instability criterion $\varepsilon \to \infty$ can be defined at a finite failure time, resulting in the localization of damage and the formation of a throughgoing fracture.

In the hybrid model, transient creep dominates in the early stages of damage and accelerating creep in the latter stages. At intermediate times the linear superposition of the two mechanisms spontaneously produces an apparent steady-state phase of relatively constant strain rate, with a power-law rheology, as observed in laboratory creep test data. The predicted acoustic emission event rates in the transient and accelerating phases are identical to the modified Omori laws for aftershocks and foreshocks, respectively, and provide a physical meaning for the empirical constants measured. At intermediate times, the event rate tends to a relatively constant background rate. The requirement for a finite event rate at the time of the main shock can be satisfied by modifying the instability criterion to having a finite crack velocity at the dynamic failure time, $dx/dt \to V_R$, where V_R is the dynamic rupture velocity. The same hybrid model can be modified to account for dynamic loading (constant stress rate) boundary conditions, and predicts the observed loading rate dependence of the breaking strength. The resulting scaling exponents imply systematically more non-linear behaviour for dynamic loading.

Key words: aftershocks, creep, earthquakes, foreshocks, rheology, rock fracture.

INTRODUCTION

The time-dependent properties of microscopically brittle rock deformation are of first-order importance for understanding the long-term behaviour of rocks in the Earth's upper crust. Traditionally, the most common way of investigating these is to carry out a static load, or 'creep', test; that is, holding a constant differential stress on a cylindrical rock sample, with a radially symmetric confining pressure, and measuring the resulting strain as a function of time. Fig. 1 shows a schematic textbook example of how such results are typically interpreted, involving three individual stages of creep, labelled transient (primary or decelerating); steady-state (secondary or constant rate); and accelerating (tertiary or unstable). The deformation may be distributed throughout the sample in the first two phases, but the phase of accelerating creep results in the eventual failure of the sample by localization of deformation onto a single plane.

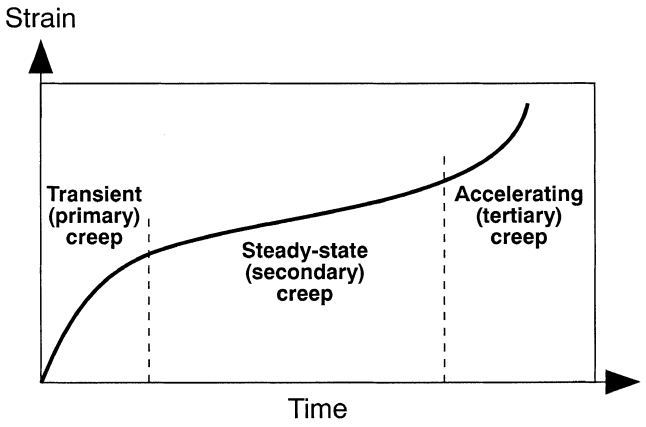

Figure 1. Schematic plot of the time-dependent strain component on a rock sample, after application of an elastic strain at time zero, redrafted after Hobbs *et al.* (1976). The behaviour separates into three phases of transient, steady-state and accelerating creep.

Classical models to explain this behaviour have included the linear superposition of a small number of viscous and elastic elements, for example the linear Burgers body (e.g. Ranalli 1995). However, all of these models exhibit a short-lived exponential transient, rather than the longer-tailed power-law transients observed in the Earth, for example Omori's law for the decay of seismic event rate in aftershock sequences discussed below. Similarly, none of these simple linear models can explain the final stage of non-linear, unstable accelerating creep, due to the progressive localization of deformation in the final stages of macroscopically brittle behaviour. In order to explain this, more complex models with very large numbers of Newtonian elastic and viscous elements are required (e.g. Davy *et al.* 1995). In such models, localization results from the co-operative behaviour of a system with a large number of degrees of freedom, with non-linearity introduced by the threshold behaviour of local failure and stress drop. In practice, we are unable to invert for such a large number of parameters based on the limited data available, although such conceptual models provide valuable insight into the processes involved in the localization of deformation.

In the mean-field theory of damage mechanics, the basic concept is a two-stage failure process, representing a transition from distributed damage by tensile microcracking, up to a critical threshold where microcracks begin to interact to form a throughgoing fracture or fault (e.g. Reches & Lockner 1994, Fig. 2). This class of model is based on laboratory observation of acoustic emissions and sample dilatancy related to microcracking during the failure of low-porosity crystalline rock in a compressive stress field (Scholz 1968a). Horii & Nemat-Nasser (1985) developed a mean field theory for this observation by considering a population of initially weakly interacting microcracks, with a transition to strong interactions and failure when the mean crack density reached a critical threshold. The stable growth of tensile microcracks in a compressive stress field is also a feature of the damage model based on analytical solutions for the development of 'wing-cracks' (including an element of local shear displacement) proposed by Ashby & Hallam (1986), Sammis & Ashby (1986) and Ashby & Sammis (1990), which includes some frictional sliding as well as a tensile component. In such models, crack growth is stabilized by stress intensity reduction at the crack tip as the crack grows. Costin (1987) reviewed the application of damage mechanics to the time-dependent failure of rock, including the case of constant stress (creep) loading. He describes models which also assume a reduction in stress intensity prior to crack interaction—for the case of axial microcracks—and includes time dependence via the rate equations for subcritical crack growth by stress corrosion. This class of model predicts the strain rate dependence of the ultimate strength and Young's modulus, typical non-linear stress–strain curves for axial and volumetric strain, and the dynamic failure time in creep experiments.

In a detailed study on granite samples at room temperature, Lockner (1993a) developed a similar model for time dependence based on stress corrosion reactions and stress intensity reduction for the 'wing-crack' model. The model results were in good agreement with experimental observations of the strain rate dependence on differential stress, and the forms of the primary and secondary creep phases. In a microstructural analysis of granite samples from an earlier test on granite samples, Moore & Lockner (1995) showed, from direct observation of microcrack statistics, that crack interactions implying a stress intensity increase only become significant very late in the secondary creep stage. This microstructural inference is consistent with the acoustic emission study of Reches & Lockner (1994), who showed that macrocrack formation inferred by planar-aligned acoustic emission (AE) locations occurred very late in the loading cycle for Westerley granite.

In order to account more accurately for the interactions leading to microcrack coalescence, Okui & Horii (1997) developed an explicit bifurcation model for the localization of a shear failure from an interaction field theory which accounted explicitly for crack interactions for both dilute and strongly interacting populations. The model, applied to a finite-element numerical grid, is also based on the assumption of stress corrosion cracking and a reduction in the stress intensity factor as the stabilizing mechanism. In accounting explicitly for late-stage positive feedback due to crack interactions, Lockner (1998) was able to obtain a good fit to the whole cycle of the creep curve in Fig. 1, including the final dynamic phase not under consideration here.

Here I develop a simpler model for the full creep cycle, and the resulting event rate for acoustic emissions or earthquakes, based on existing non-linear constitutive rules for time-dependent subcritical crack growth, combined with local hardening and softening feedback mechanisms from fracture mechanics. In the tradition of damage mechanics, the model involves the linear superposition of local negative and positive feedback of crack growth, leading to local hardening and softening, respectively, associated with two characteristic time constants. At short times the transient phase dominates, resulting in stable deformation. At long times the accelerating phase dominates, resulting in the localization of deformation onto a 'system-sized' crack. This transition occurs via a long phase of apparent 'steady-state' creep, which is not assumed *a priori*. The steady-state creep phase has a power-law rheology between the applied stress and the resulting strain rate, as observed. The predicted AE event rate follows a form similar to that of laboratory experiments, and reduces exactly to the modified Omori law for earthquake aftershock and foreshock sequences, with an intervening 'background' rate due to the

superposition of the two processes. The main advantage of the constitutive rules obtained here over the models discussed above is their analytical simplicity, making it easier in principle to fit the model to data from the laboratory and the field. In addition, power-law creep is an emergent property of the model, rather than a constraint.

The same model is then applied to the case of dynamic loading at a constant rate. This decreases the predicted failure time compared with conditions of static loading, and produces a more rapid acceleration in the final stages of failure, given the same material constants. The model predicts a non-linear dependence of breaking strength as a function of loading rate, as observed in constant strain rate experiments, and in particular provides a better fit at low strain rates than alternative models that ignore the finite threshold for subcritical crack growth. A similar two-stage evolution for the AE event rate is also predicted, as observed by Liakopoulou-Morris *et al.* (1994).

Positive and negative feedback in crack growth

The Griffith criterion for unstable crack growth can be derived from the field of linear elastic fracture mechanics. In this formulation, the criterion for crack growth can be expressed as a function of the stress intensity K at the tip of a crack of half-length x, resulting from an applied stress σ at a remote boundary, which we will write in the general form

$$K = Y\sigma x^q, \tag{1}$$

where the constant Y depends on the loading configuration and the mode of failure. The crack will grow stably for a finite increment when $\partial K/\partial x < 0$ (Lawn 1993, eq. 2.3), or $q < 0$. Thus negative q corresponds to stress intensity reduction as a function of increasing crack length. Such negative feedback may arise from the external loading conditions, or from local stress relaxation or hardening mechanisms at the crack tip. In contrast, unstable crack growth occurs when $\partial K/\partial x > 0$, or $q > 0$. This positive feedback introduces a fundamental non-linearity that results in accelerating crack growth. In the classical Griffith crack loading conditions, $q = 1/2$, $Y = \sqrt{\pi}$, and instability occurs when $K > K_c$, where the critical stress intensity K_c is known as the fracture toughness. Lawn (1993) also describes examples of external loading conditions in laboratory tests on ideal, homogeneous materials where $q = 0$ (no feedback), and $q = -1/2$ (negative feedback) for the case of a single crack. For a crack *population*, the effective value of q will be an average over a population at different stages of growth, corresponding to different local values of q which may itself be a function of crack length (e.g. Ashby & Hallam 1986). Here q is therefore allowed to take on a continuum of values that need not be $i/2$, where i is an integer.

The behaviour described so far, assuming vacuum conditions and material homogeneity, is time-independent. However, ceramic materials (including rocks and minerals) are both heterogeneous and porous, making them sensitive to stress-enhanced chemical reactions with the interstitial pore fluid, and also to local negative feedback processes due to stress relaxation or dilatancy hardening on the grain scale. Such 'internal' negative feedback can result from stabilizing changes in pore volume which may accommodate the strain without requiring further crack growth (Horii & Nemat-Nasser 1985; Ashby & Hallam 1986; Costin 1987). Chemical (stress corrosion) reactions also allow crack growth to occur at stress intensities below K_c, at a velocity that is non-linearly dependent on K. Experimental data for subcritical crack growth in rocks, minerals and ceramics can often be fitted to the power-law form of Charles' law:

$$\frac{dx}{dt} = V_0\left(\frac{K}{K_0}\right)^n; \qquad K_{\min} < K < K_c, \tag{2}$$

where V_0 is the starting velocity at time $t_0 = 0$, K_0 is the initial stress intensity at time t_0, and the exponent n—a quantitative measure of the non-linearity of the chemically assisted process of crack growth—is known as the stress corrosion index (e.g. Atkinson & Meredith 1987). Typically, n varies experimentally between 20 and 50 for crack growth by stress corrosion in ceramic materials (Atkinson & Meredith 1987), and takes on the value $n = 30$ for basalt. The presence of a thermally activated chemical weakening processes introduces a minimum stress intensity $K_{\min}$ below which the velocity of crack growth is zero or negative (Rice 1978). For a given initial maximum crack length, x_0, representing the typical initial flaw size in the material, this implies a minimum stress $\sigma_{\min} = K_{\min}/(Yx_0^q)$ for the activation of the subcritical crack growth mechanism. Thermal processes change this minimum stress, but not the exponent n, which is more sensitive to the chemical environment (e.g. Atkinson & Meredith 1987).

In order to solve the first-order differential equation (2), given (1), we need to know the stress history $\sigma(t)$. The two main types of laboratory test involve either *static fatigue* (constant load or 'creep' test), or *dynamic fatigue* (constant strain rate). In theoretical treatments, it is often more convenient to solve the relevant equations by assuming constant stress rate loading (e.g. Sano *et al.* 1981; Costin 1987), implicitly assuming a constant elastic modulus. Since we are interested in first-order properties, we follow the latter approach for the case of dynamic loading here, but acknowledge that modifications will be necessary when there are strong deviations from linearity in the modulus (Lockner 1998).

Static loading (creep test)

In this section I first describe how secondary creep emerges as a consequence of the linear superposition of the two processes of stable and unstable crack growth due to local negative and positive feedback. The model is then used to derive a relationship between the exponents for subcritical crack growth and the power-law rheology of the emergent steady-state phase. I also show how the modified Omori law for foreshock and aftershocks sequences can be derived from the same theoretical treatment.

(a) Time-dependent crack growth

The boundary condition for creep during constant stress loading is $\sigma(t) = \sigma_0 > \sigma_{\min}$, whence the general solution of (1) and (2) takes the form

$$x = x_0[1 + t/(m\tau)]^m; \qquad m \neq 0, \tag{3}$$

where

$$m = (1 - nq)^{-1}, \qquad \tau = x_0/V_0 \tag{4}$$

[see Das & Scholz (1981) for the case $q = 1/2$, or equivalently $m = 2/(2-n)$]. Here x_0 and V_0 are the starting crack length and velocity, respectively. For $\sigma(t) < \sigma_{\min}$ there is no time-dependent crack growth, and $x(t) = x_0$. For the special case $m = 0$, an exponential dependence is predicted (Main 1999).

Eq. (3) holds for the specific case of crack length increase. However, it is also a solution to Voight's (1988, 1989) more general second-order differential equation for precursory strain Ω, in a material undergoing damage in the form of a crack population, of the form

$$d^2\Omega/dt^2 - a(d\Omega/dt)^{\alpha} = 0, \tag{5}$$

where a is a constant, and α is an exponent which measures the degree of non-linearity (related in turn to a globally averaged value of m). Strain may be measured directly, using strain gauges in laboratory tests, or satellite or geodetic studies for crustal strain. In situations where direct measures are not available it is common to use a proxy measure of strain, often based on the properties of a population of earthquakes, the most appropriate of which is the sum of moment tensors using the definition provided by Kostrov (1974), as discussed in Main (1999).

Voight's equation has a general solution,

$$\Omega = \Omega_0[1 + t/(m\tau)]^m; \qquad m \neq 0, \tag{6}$$

identical to the form of eq. (3) and also for a simple percolation model for time-dependent crack growth (Main 1999). From this comparison, we expect the same analytical form to hold for measured strain and crack length, although we would not expect m to be the same. The precise value of m will depend on the dependence of stress intensity on crack length (expressed by the parameter q), and on the effect of averaging over a population of many cracks that may be of different lengths. When considering the effect of a *population* of cracks, it is more appropriate to use eq. (6), with strain as the appropriate variable.

When $m < 0$, the general solution takes the special form

$$x = x_0[1 - t/t_f]^m; \qquad t_f = -m\tau, \qquad m < 0. \tag{7}$$

The presence of a negative sign in the term in square brackets changes the behaviour completely. This results in a quasi-static instability that can be expressed in two commonly derived forms. The first criterion uses the approximation $x, dx/dt \to \infty$ as $t \to t_f$, resulting in the localization of damage onto a 'system-sized' (effectively infinite) fault at the failure time t_f. Alternatively, instability may be defined when the velocity of crack growth approaches the inertial limiting rupture velocity $dx/dt \to V_R$, whence

$$x = x_0[1 - t/(t_f - t^*)]^m, \qquad m < 0, \tag{8a}$$

where

$$t^* = -m\tau(V_0/V_R)^{[1/(1-m)]}. \tag{8b}$$

In this case, the failure occurs earlier ($dx/dt = V_R$, *cf.* $dx/dt = \infty$), and the crack length remains finite at the failure time, hence preserving finite strain. For the usual case $V_R \gg V_0$, $m < 0$, $t^* \approx 0$, and (8) reduces to the form (7). Thus we expect t^* to be a small correction compared with the absolute magnitude of the failure time, although a finite t^* is required to keep the crack length finite at $t = t_f$. In laboratory tests an additional source of dynamic instability occurs when the fault weakening rate becomes comparable with the elastic unloading rate of the surrounding material, thereby increasing t^* further.

The general form of eq. (3) implies that the quasi-static stability/instability conditions for time-dependent crack growth (irrespective of whether strain or crack length is used as the measured variable) depend on the sign of m, which in turn depends on the values of both q and n. In the case of no feedback ($q = 0$), $m = 1$ for all values of n, and eq. (3) predicts crack growth at a constant rate $x = x_0/\tau$. For positive feedback ($q > 0$), there are two regimes of behaviour. For $nq > 1$, the instability criterion $m < 0$ holds, and eq. (7) can be used to a good approximation. For $nq < 1$, $m > 1$, and crack growth according to eq. (3) is accelerating but stable, in the sense that there is no system-sized event. Finally, for a negative feedback process ($q < 0$), eq. (4) predicts $0 < m < 1$, and stable, decelerating crack growth according to eq. (3).

(b) The hybrid model

It is possible to use the above theory to develop a three-stage model for the three phases of creep seen in Fig. 1. This involves a linear superposition of three distinct processes with exponents $0 < m_1 < 1$, $m_2 = 1$, $m_3 < 0$; timescales T_1, T_2 and t_f; and initial weights Ω_I, Ω_{II}, Ω_{III}, where $\Omega_I + \Omega_{II} + \Omega_{III} = \Omega_0$, and Ω_0 is the total elastic strain at time zero. However such a model requires nine independent parameters and it is not clear whether a separate distinct mechanism is required for secondary creep (Varnes 1983; Lockner 1998). In damage mechanics it is typical to assume a two-stage process involving initial negative feedback due to local hardening processes, and later positive feedback due to crack interactions (see discussion in the Introduction). We therefore consider a linear superposition of only two different processes, based on the general forms of the constitutive rules for subcritical crack growth discussed above. The model parameters are then the time constants τ_1 and τ_3, respectively, for the processes of stable, transient creep associated with negative feedback and local material hardening ($0 < m_1 < 1$), and unstable, accelerating creep associated with positive feedback and material weakening ($m_3 < 0$). In order to keep all parameters positive we define $v = -m_3$, and for convenience drop the subscripts for T_1 and m_1. The resulting hybrid model for the measured strain due to a crack population has the form

$$\Omega = \Omega_I[1 + t/T]^m + \Omega_{III}[1 - t/t_f]^{-v}, \tag{9}$$

where $T = m\tau_1$, $t_f = v\tau_3$, and the sum of the constants $\Omega_I + \Omega_{III} = \Omega_0$, that is, the elastic strain applied at time zero. This equation is based on a linear superposition of solutions that independently satisfy (5), so it is also a solution to (5). The model then requires only six independent parameters, one of which is the (fixed) elastic strain, and the remaining five describe the inelastic strain. A more complex fit to actual data would have to be justified in terms of a finite penalty for the extra number of parameters required (e.g. Main *et al.* 1999).

An example of a calculation of the total strain from eq. (9) is given in Fig. 2 (a), for $\Omega_I = \Omega_{III} = \Omega_0/2$, with $\Omega_0 = 1$, $m = 0.2$, $v = 0.2$, $T = 0.05$ and $t_f = 1$. The graph shows both the individual components and the sum, all normalized to unit initial strain for comparison. The shape of the hybrid curve follows the classical curve in Fig. 1. There is an early phase dominated by

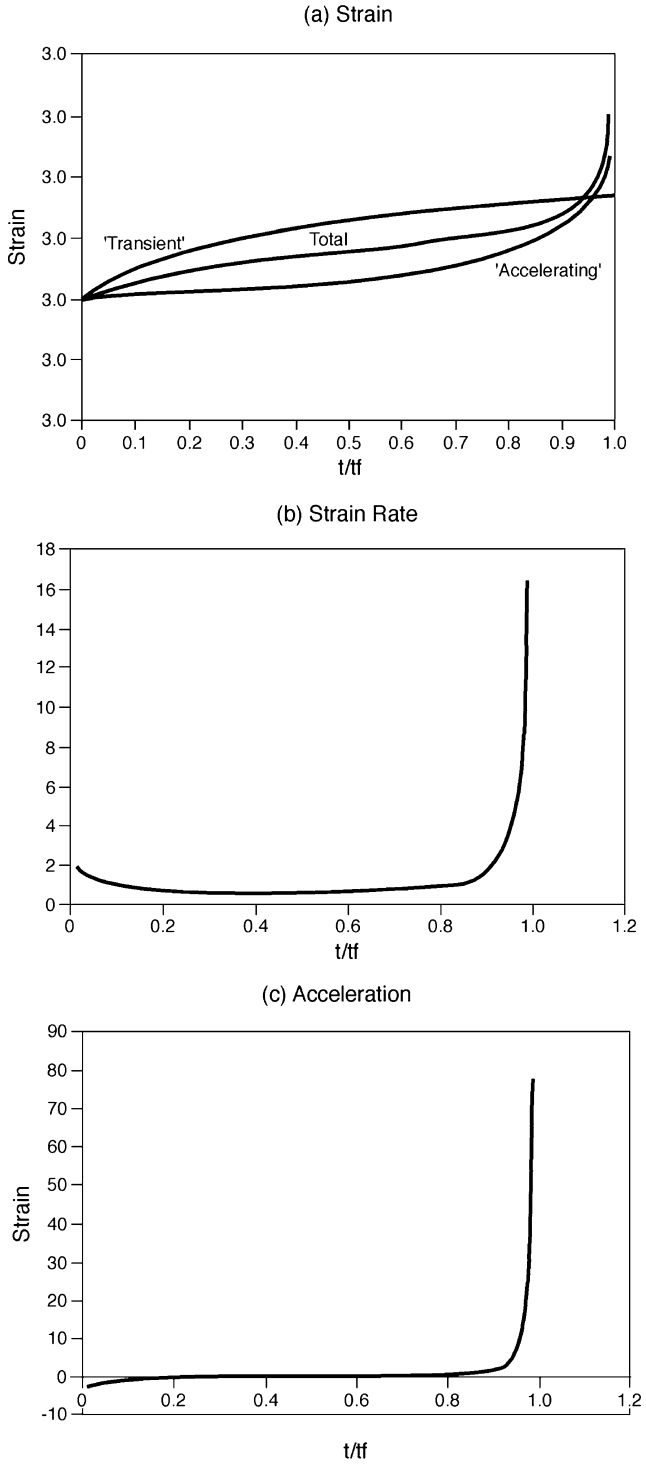

Figure 2. (a) Strain versus time plot for eq. (9), showing the individual components of transient and accelerating creep, as well as the total, all shown on normalized units for comparison. (b) Strain rate versus time from eq. (12). (c) Strain acceleration versus time from the equation obtained from differentiating eq. (9) twice. In all plots the values of the parameters are $m = 0.2$, $v = 0.2$, $\Omega_{\rm I} = \Omega_{\rm III} = 1/2$, $T = 0.05 t_{\rm f}$.

transient creep, a final phase dominated by accelerating creep leading to instability, and most importantly, since it was not an *a priori* assumption of the model, an intermediate phase of apparent steady-state creep.

(c) Derivation of Omori's law for foreshocks and aftershocks

It has long been recognized that acoustic emissions due to microcracking in the laboratory could provide a useful analogue for the examination of earthquake foreshock and aftershock sequences (Scholz 1968b; Lockner 1993b). However, the straining mechanism in the laboratory for crystalline rocks occurs by local dilatant microcracking, and natural seismicity occurs by shear on pre-existing faults, so the quantitative behaviour may be significantly different in detail. For example, laboratory tests typically produce more foreshocks than aftershocks, contrary to the case observed in seismicity data. In this section the specific model developed above is related quantitatively to the occurrence of foreshocks and aftershocks.

The modified Omori law for earthquake aftershocks is described in terms of the time dependence of the seismicity rate $R_{\rm a}$, which has the form

$$R_{\rm a} \sim (c_{\rm a} + t - t_{\rm M})^{-p}, \tag{10}$$

where $c_{\rm a}$ is a constant and $t_{\rm M}$ is the time of the main shock (Utsu *et al.* 1995). A similar behaviour has also been proposed for foreshocks:

$$R_{\rm f} \sim (c_{\rm f} + t_{\rm M} - t)^{-p'}, \tag{11}$$

where the subscript f here refers to foreshocks, and p' is the exponent for foreshocks. This rate law has been determined from a statistical analysis involving the superposition of data, and carried out in retrospect, because of the difficulty in identifying such a law in prospective mode from individual foreshock–mainshock sequences (Kagan & Knopoff 1978). Both p and p' are positive, and are found empirically to be close to 1 (Utsu *et al.* 1995; Hainzl *et al.* 1999).

In order to determine the rate dependence, we differentiate eq. (9), to obtain

$$\dot{\Omega} = \frac{m\Omega_{\rm I}}{T}[1 + t/T]^{m-1} + \frac{v\Omega_{\rm III}}{t_{\rm f}}[1 - t/t_{\rm f}]^{-v-1}. \tag{12}$$

This can be regarded as a general equation for the seismic event rate because of the observation of proportionality between AE event rate R and crack velocity V: $R = \alpha V$ (Meredith & Atkinson 1983). The form of eq. (12) assumes loading at time $t_0 = 0$. Using the proportionality between event rate and crack growth rate, and making the timescale arbitrary relative to a starting time t_0, eq. (12) reduces with some manipulation to

$$R = \frac{\alpha m\Omega_{\rm I}}{T^m}[T + (t - t_0)]^{m-1} + \frac{\alpha v\Omega_{\rm III}}{(t_{\rm f} - t_0)^{-v}}[t_{\rm f} - t]^{-v-1}. \tag{13}$$

This equation holds for the definition of failure time given above for an infinite crack velocity at $t = t_{\rm f}$. In order to match the observed finite event rate at the time of the main shock, define $t = t_{\rm M}$ when $dx/dt = V_{\rm R}$, with $V_{\rm R}$ finite according to eq. (8). In this case (13) reduces to

$$R = \frac{\alpha m\Omega_{\rm I}}{T^m}[T + t - t_0]^{m-1} + \frac{\alpha v\Omega_{\rm III}}{(t_{\rm M} + t^* - t_0)^{-v}}[t_{\rm M} + t^* - t]^{-v-1}, \tag{14}$$

where t^* is defined in eq. (8b). The first term describes the occurrence of aftershocks in the same form as (10), with

$R_a = \alpha m \Omega_I / T^m$, $T = c_a > 0$, $p = 1 - m$, and t_0 the time of the previous main shock. The second term describes the occurrence of foreshocks as in (11), with $R_f = \alpha v \Omega_{III} / (t_M + t^* - t_0)^{-v}$, $t^* = c_f > 0$ and $p' = 1 + v$. Although the functional forms of (10) and (11) appear very similar, we note from (14) that the origins of the two terms c_a and c_f are completely different. $c_a = T$ results directly from the time constant $\tau_1 = T/m$ from the general solution to eqs (1) and (2) for local negative feedback ($0 < m < 1$). The constant term c_a is typically of the order of 0.5 days (e.g. Reasenberg 1999). The negative feedback here may be related to the local stress relaxation during aftershocks, or to time-dependent healing in the post-seismic phase. In contrast, $c_f = t^*$ results from the requirement of a finite rupture velocity at the time of the main shock for local positive feedback ($v > 0$). Small positive values for both m and v can be inferred from the empirical observation that p and p' are both near 1. This implies that earthquake behaviour is more non-linear than other types of critical-point phenomena, where the exponent v is of the order of 0.6–1 (Stanley 1971, Table 3.4).

The predicted behaviour of strain rate (eq. 12), or AE event rate (eq. 14), for a laboratory creep test, or the interseismic period between two main shocks, is shown in Fig. 2(b), using the same parameters as in Fig. 2(a). The AE rate is predicted to decay according to a power law with exponent $m - 1 < 0$, to a relatively flat 'background' level, before accelerating once more to a maximum at the dynamic failure time. A major difference between earthquake data and laboratory data is the greater relative proportion of foreshocks (accelerating strain phase) than aftershocks (decelerating strain phase) in laboratory experiments. This may be accounted for in a straightforward way by differences in the model parameters, either via the weights $\Omega_{I,III}$, or the exponents m and v. In particular, laboratory tests show a more gradual acceleration of seismic event rate up to the dynamic failure time (Liakopoulou-Morris *et al.* 1994), implying a significantly larger value of v compared with $v \approx 0$ inferred for earthquake foreshocks discussed above. This implies that the appropriate constitutive rule for the final stage of earthquake occurrence is more non-linear than that often found in the laboratory. A more precise comparison is given in the discussion.

Fig. (2b) clearly shows that the strain rate during 'secondary' creep is not actually constant in any part of the secondary phase, although with a degree of statistical noise a good fit is likely to be obtained to a flat line in this part. The power-law decay results in a fatter 'tail' than the corresponding exponential transient predicted by the Burgers model, and leads to significant mixing of the two distributions in the middle range. Quite often, laboratory results for measured acoustic emissions have been interpreted with this 'background' phase interpreted as ambient noise. Here the finite 'background' seismicity during secondary creep is a 'signal' that occurs due to the combination of two processes with long tails. This signal may be missed if the acoustic threshold for recording is set too high, or if the ambient signal-to-noise ratio in the laboratory or field is less than one.

Finally, the acceleration calculated from the second derivative of eq. (9) is shown in Fig. 2(c). In this case, the distinction between the three phases is most evident, with a long flat phase of nearly zero acceleration corresponding to apparent steady-state creep, but produced as a result of the superposition of two non-linear processes with time constants T and t_f. We conclude that a hybrid process can give a good explanation for the emergence of secondary creep, requiring five independent parameters for the inelastic component, and producing a transient creep phase consistent with the modified Omori law for aftershock and foreshock sequences.

(d) The emergence of a 'power-law' rheology for steady-state creep

Eq. (1) suggests a possible relationship between the exponent n for subcritical crack growth and the exponent η for power-law creep, which takes the form

$$\dot{\Omega} = A\sigma^{\eta}, \tag{15}$$

where $\dot{\Omega}$ is the strain rate and A is a constant. A full analytical derivation of (15) from (12) is not possible in the general case, although for the purposes of illustration this is undertaken here with some simplifying assumptions. The strain rate in the steady-state phase is estimated by taking $\Omega_I = \Omega_{III} = \Omega_0/2$ as before, and assuming a constant ratio $r = T/t_f$. The slope of the strain rate during this phase is reasonably constant in the middle part of the curve (Fig. 2), so the strain rate during secondary creep is estimated at time $t = t_f/2$. In this case, eq. (10) predicts that the strain rate is

$$\dot{\Omega}(t_f/2) = \frac{\Omega_0}{2t_f}\{m[1 + 0.5/r]^{m-1} + v[1 - 0.5]^{-v-1}\} = \text{const}\ \frac{\Omega_0}{t_f}. \tag{16}$$

Eq. (2) holds for any starting stress $\sigma_0 \geq \sigma_{min}$, so that $V_0/K_0^n = V_{min}/K_{min}^n$, or $V_0 = V_{min}[(Y\sigma_0 x_0^q)(Y\sigma_{min} x_{min}^q)]^n$ from (2). Since the geometric factor Y is constant, and the starting flaw size x_0 is the same for any starting stress, the failure time is then

$$t_f = v\frac{x_0}{V_0} = v\frac{x_0}{V_{min}}\left(\frac{\sigma_0}{\sigma_{min}}\right)^{-n}; \qquad \sigma_0 \geq \sigma_{min}, \tag{17}$$

where the subscripts 0 refer to zero time, and the subscript min refers to the minimum or threshold value for subcritical crack growth at a finite velocity. V_{min} is assumed to be a constant for a given fluid–rock system. Fig. 3 shows the predicted curve for the hybrid model for three values of t_f, and hence σ_0, each normalized to the starting strain, given the assumptions above. From (16) and (17), the ratio of strain rates during the period of steady-state creep for starting stresses σ_0 and σ_{min} is then

$$\frac{\dot{\Omega}(t_{II})}{\dot{\Omega}_{min}} = \frac{\Omega_0}{\Omega_{min}}\frac{t_f^{min}}{t_f} = \frac{\Omega_0}{\Omega_{min}}\left(\frac{\sigma_0}{\sigma_{min}}\right)^{n}. \tag{18}$$

For the elastic phase the stress σ is proportional to the strain Ω, so

$$\frac{\dot{\Omega}(t_{II})}{\dot{\Omega}_{min}} = \left(\frac{\sigma_0}{\sigma_{min}}\right)^{n+1}; \qquad \sigma_0 \geq \sigma_{min}, \tag{19a}$$

$$= 0; \qquad \sigma_0 < \sigma_{min}. \tag{19b}$$

Eq. (19a) is identical to (15) for

$$A = \dot{\Omega}_{min}/\sigma_{min}^{n+1}, \tag{20}$$

and

$$\eta = n + 1. \tag{21}$$

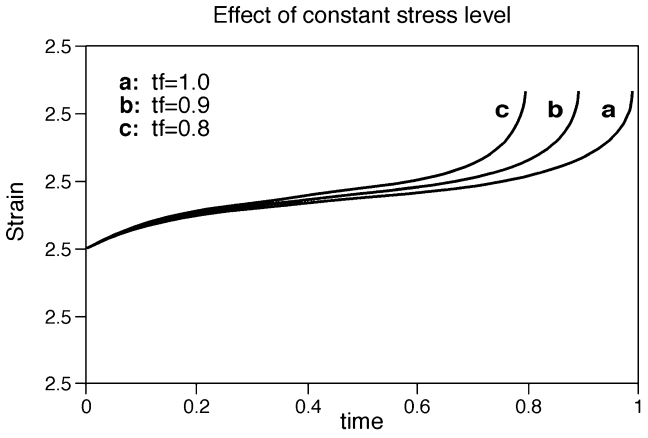

Figure 3. Plot of the acceleration of strain to failure from differentiating eq. (9) twice for various values of t_f. In each case the strain is normalized to its starting value. As the failure time decreases, or equivalently the starting stress increases, the slope in the apparently 'steady-state' phase increases. The rate of this increase as a function of stress forms the basis for the power-law creep rheology.

These relations apply strictly to the set of simplifying assumptions stated above. In the more general case, the constant term in (16) is not appropriate, and a numerical solution is required, given appropriate input for the distribution parameters from curve fits to time-dependent strain data.

For normal laboratory experiments on single crystals, it is sometimes possible to measure the minimum crack velocity for subcritical crack growth (e.g. Lawn 1993). However, for polycrystalline aggregates, the strain rate is always much faster than the minimum strain rate needed to promote subcritical crack growth (Atkinson & Meredith 1987). To examine the behaviour in this case we rearrange equation (19a) in the form

$$\sigma_0 - \sigma_{\min} = \sigma_{\min}\left\{\left(\frac{\dot{\Omega}(t_{II})}{\dot{\Omega}_{\min}}\right)^{1/(n+1)} - 1\right\}. \tag{22}$$

For the case of strain rates that are rapid compared to the threshold strain rate $\dot{\Omega}(t_{II})/\dot{\Omega}_{\min}(t_{II}) \gg 1$, so this reduces to

$$\frac{\dot{\Omega}(t_{II})}{\dot{\Omega}_{\min}(t_{II})} = \left(\frac{\sigma_0 - \sigma_{\min}}{\sigma_{\min}}\right)^{n+1}, \tag{23}$$

or

$$\dot{\Omega}(t_{II}) = A(\sigma_0 - \sigma_{\min})^n, \tag{24}$$

where η and A are as defined above. Eq. (24) is currently being fitted to steady-state creep test data on sandstones of varying strength and cohesion.

Constant stress rate (dynamic) loading

I now consider the effect of loading in the form of a stress or strain ramp of the form

$$\sigma(t) = \dot{\sigma} t, \tag{25}$$

where the dot indicates a first derivative with respect to time. Since the starting stress is now zero, it is necessary to take explicit account of the finite threshold for subcritical crack growth (e.g. Lawn 1993).

(a) Time-dependent strain

The conditions for crack growth with a finite threshold are

$$\dot{x} = 0; \qquad t < t_{\min}, \tag{26a}$$

$$\dot{x}(x_{\min}/x)^{nq} = V_{\min}\left[\frac{\dot{\sigma} t}{\sigma_{\min}}\right]^n; \qquad t \geq t_{\min}, \tag{26b}$$

where $t_{\min} = \sigma_{\min}/\dot{\sigma}$ is the time when the stress is sufficiently high to activate the stress corrosion mechanism. At this time, the starting velocity, crack length and stress take on their minimum values (e.g. Lawn 1993). Before then there is no crack growth. A general solution relevant for either case can be obtained by the substitution $y = t/t_0$, $dy/dt = t/t_0$, and integrating as before to give, for $m \neq 0$,

$$x = x_0; \qquad t < t_0, \tag{27a}$$

$$x = x_0\left\{1 + \left(\frac{1}{m(n+1)}\right)\left(\frac{V_0 t_0}{x_0}\right)\left[\left(\frac{t}{t_0}\right)^{n+1} - 1\right]\right\}^m; \qquad t \geq t_0. \tag{27b}$$

This exact solution replaces the approximation derived in Main (1988). There are two sources of non-linearity here, one from the exponent m of the term in curly brackets, $m = [1 - qn]^{-1}$, i.e. identical to that found for constant stress loading, and one from the non-linearity in time t introduced as an exponent into the term within the curly brackets. For $m < 0$, $qn > 1$, the crack grows without limit when the term in curly brackets in (27b) becomes zero, or when

$$t = t_f = t_0\left\{1 + m(n+1)\left(\frac{x_0}{V_0 t_0}\right)\right\}^{1/(n+1)}; \qquad m < 0. \tag{28}$$

The normalized failure time, t_f/t_0, and the rate of acceleration to failure depend on the value of the exponents q and n, and on the ratio of the characteristic times τ/t_0. The time constant $\tau = x_0/V_0$ is inversely proportional to the reaction rate for the initiation of subcritical crack growth, and t_0 is inversely proportional to the loading rate. Fig. 4(a) shows the behaviour for eq. (27) (curve A), compared with that for eq. (3) (curve B), for the case $v = 1$, normalized to the same failure time. In curve A, crack growth only starts at time $t_0 = 1$, whereas for B it begins immediately on loading. Apart from this threshold effect, the main difference is that eq. (27) is more non-linear, resulting in a curve A that resembles the constant stress curve B, but with an apparently smaller apparent exponent v. In earthquake foreshock sequences, with a finite loading rate, this correction leads to more non-linear behaviour than for the case of constant load, consistent with the apparently lower value of v inferred above from field data.

In practice it may be hard to discriminate on statistical grounds between eqs (3) and (27), because both show very similar non-linear divergence near the failure time, and because of the paucity of foreshocks generally. In the laboratory, however, it might be feasible to attempt such a discrimination for controlled tests at different finite loading rates. The predicted difference between the two types of behaviour (constant load and constant loading rate) from eqs (3) and (27) is shown

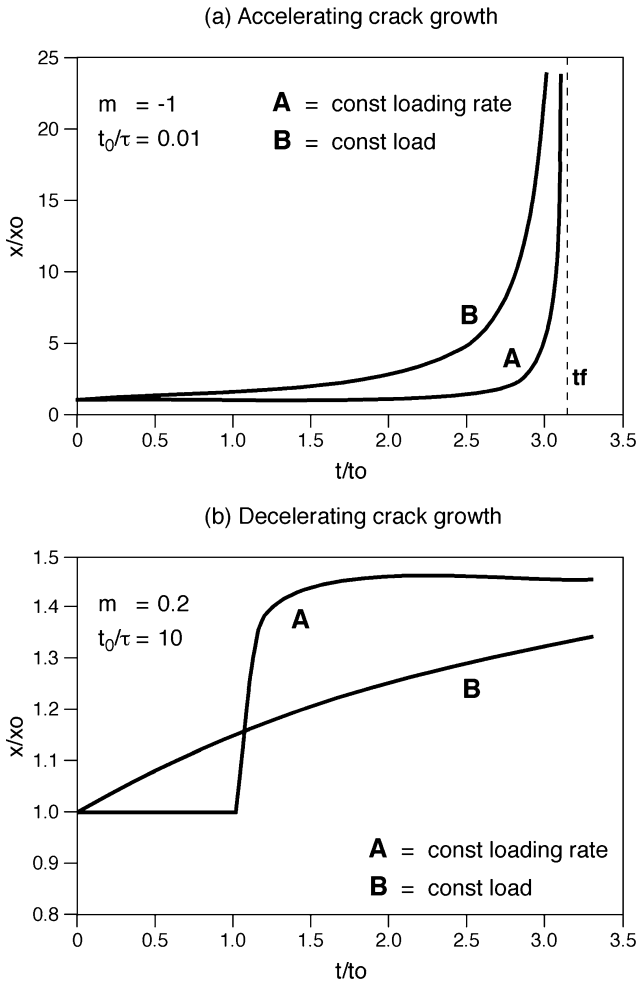

Figure 4. Plot of normalized crack length x/x_0 versus normalized time $t/t_0 - 1$, for A constant loading rate (eq. 27), and B constant load (eq. 3) for the case of a finite failure time.

for the transient creep phase in Fig. 4(b). The effect of constant loading rate is to introduce a threshold, and to increase the non-linearity in the curve for transient or decelerating creep ($m = 0.2$ assumed in both curves). The effect of dynamic loading is therefore to increase the rate of acceleration in the tertiary phase.

(b) Rate dependence of failure strength

Eq. (28) can be used to predict the loading rate dependence of the breaking strength (stress at time t_f), from

$$\sigma_f = \dot{\sigma} t_f = \sigma_0 \left[1 + m(n+1) \left(\frac{\dot{\sigma}\tau}{\sigma_0} \right) \right]^{1/(n+1)} . \qquad (29)$$

The predicted curve is shown in Fig. 5 for the case $v = 1$. For high loading rates, $\tau\dot{\sigma}/\sigma_0 \gg 1$, this reduces to

$$\log(\sigma_f) = \frac{1}{n+1} \log(\dot{\sigma}) + D , \qquad (30)$$

where D is a constant. This is identical to forms suggested by Sano *et al.* (1981), and Lankford (1981).

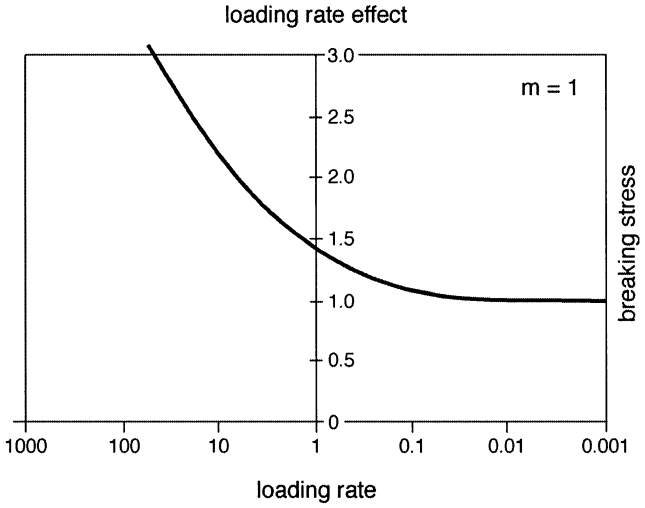

Figure 5. Plot of normalized breaking strength σ_f/σ_0 as a function of loading rate for the case $v = 1$; $\dot{\sigma}\tau/\sigma_0 = 1$, from eq. (29).

The main difference between (29) and (30) is at small loading rates, where the breaking stress reaches a finite threshold stress σ_0 asymptotically. In fact, some of the plots of data from uniaxial compression tests reported in Sano *et al.* (1981, Fig. 11) do show evidence of such asymptotic curvature at low stress rates, and hence were not included in the curve fits to eq. (31) in that paper. Equivalent strain rates for the laboratory tests in Sano *et al.* (1981, Fig. 11) are between 10^{-9} and $10^{1}\ s^{-1}$, with only the lowest strain rate data showing some evidence of threshold effects. However, this is likely to be more significant for the lower strain rates that pertain to the deformation of the Earth's brittle crust, resulting in a finite residual strength even after geological time periods.

The alternative damage model summarized by Costin (1987, Fig. 5.15) also has a finite threshold for low strain rates, but does not accurately predict the curvature observed in the data used to validate the model (Costin 1987, Fig. 5.15), or that of Sano *et al.* (1981, Fig. 11). Eq. (29) therefore accounts for the observed deviations between the data and the observations in either case, preserving the threshold nature of the model of Costin (1987) at low strain rates, and the power-law scaling observed by Sano *et al.* (1981) at high strain rates in a single model.

For the case where $t \gg t_0$, The predicted strain for the hybrid model, with a transition from distributed to localized damage as above, would then take the form

$$\Omega = \Omega_I [1 + (t/T)^{[3-(2/m)]}]^m + \Omega_{III} [1 - (t/t_f)^{[3-(2/v)]}]^{-v} , \qquad (31)$$

with all parameters positive as before. Again, a reasonable fit to eq. (9) might be obtained, but with smaller apparent values of v and m (e.g. see Fig. 4a).

DISCUSSION

Comparison of laboratory and field exponents

The results presented here show that the type of crack growth depends both on the feedback parameter q and on the material constant measuring the degree of non-linearity in crack growth

n. The results can be generalized to a population of cracks, since they also satisfy Voight's more general equation for strain, albeit with different magnitudes of the exponents, and requiring mean field values for q which allow for variations in crack length and positive or negative interactions between individual cracks. This approach differs from previous damage models which assume $q = 1/2$ *a priori*, and project local stress shielding effects into variations in the stress corrosion index (Liakopoulou-Morris *et al.* 1994; Renshaw & Park 1997) in two-stage models for the growth of a crack population. In particular, the transition from $n < 2$ to $n > 2$ observed in the AE data for a dynamic loading experiment in Liakopoulou-Morris *et al.* (1994), assuming $q = 1/2$, can be generalized to a transition from $nq < 1$ to $nq > 1$, or from $m > 0$ to $m < 0$ in eq. (3). This previously observed transition from stable to unstable damage is therefore exactly consistent with the hybrid model proposed above, appropriately modified to take account of the dynamic loading boundary conditions. In detail, the data of Liakopoulou-Morris *et al.* (1994, Fig. 8) show a transition from a stable crack growth phase with $nq \approx 0.7$ to an unstable phase with $nq \approx 2.5$. If we consider that $n > 10$ is a likely 'true' value for the stress corrosion index (Atkinson & Meredith 1987), then these laboratory results correspond to $q < 0.7$ for stable crack growth, and to $0.7 < q < 0.25$ for unstable crack growth. The small but positive value of q implies a reduced positive feedback ($0 < q < 0.5$) for these tests, rather than $q < 0$ assumed in the various creep models described above, including the one presented here. The most likely physical reason for this difference is that the finite loading rate in this case more than compensates for the decrease in stress intensity in a particular growth increment. For the experiments of Liakopoulou-Morris *et al.* (1994) $v > 2.5$, a value much greater than that assumed for earthquake foreshock sequences, $v \approx 0$, discussed above. This implies that earthquake foreshock occurrence accelerates more rapidly as $t \to t_M$ than the acceleration of event rate in the laboratory. The low absolute value of v inferred for foreshock sequences is also low compared to that for any critical phenomenon (Stanley 1971).

Alternative models

The model presented here is not the first to show that steady-state creep may not be an intrinsic process, but rather results from a superposition of different local processes. Varnes (1983) derived a form based on the special solution to (1) and (2), for $q = 1/2$ and $m < 0$, for both processes. This assumption has the rather unphysical consequence of requiring the timescale to be reversed in the transient phase (as plotted in Bufe & Varnes 1993). In contrast, the general solution provided here predicts the full range of behaviour in an internally consistent way, and also predicts emergent properties not considered by Varnes (1983).

In a more comprehensive analysis than presented here Lockner (1998, Fig. 10) also used the constitutive rules for subcritical crack growth, combined with a stress intensity reduction mechanism at the crack tip, to predict the three stages of creep in Fig. 1 for the case of Westerley Granite. In his model steady-state creep is also an emergent process, occurring in a region where the processes of microcrack growth and fault nucleation exactly balance. His model includes an explicit instability criterion for dynamic failure, namely when the fault weakening rate equals the elastic unloading rate of the surrounding material. This in turn predicts the sudden and dynamic increase in strain rate observed at the dynamic failure time, in a more realistic way than the quasi-static model presented here.

Lockner's (1998) model can be applied to a wide range of experimental protocols, and requires two additional free parameters for the behaviour at different confining pressures. Like Costin (1987) and Lawn (1993), he assumes an exponential form for stress corrosion crack growth rather than the power-law form (eq. 2) used here, and hence his predicted strain rate dependence on the differential stress is an exponential rather than a power law. A similar result can be obtained here by replacing Charles' law with the reaction rate equation, although this is not carried out explicitly here. This question is important, since the reaction rate theory gives a better theoretical match to the exponential strain rate dependence on stress predicted by time-dependent dynamic friction models (e.g. Dieterich 1978; Ruina 1983). Ruina (1983) writes the constitutive rule in the form

$$\tau = \sigma[\mu_0 + \theta + A \ln(V/V_c)], \tag{32a}$$

$$d\theta/dt = (-V/d_c)[\theta + B \ln(V/V_c)], \tag{32b}$$

where τ is the shear stress, σ is the normal stress, μ_0 is the static coefficient of friction, θ is the state variable representing the history of indentation healing, V is the sliding velocity, proportional to the strain rate on the fault, d_c is the critical slip distance for velocity-weakening friction, V_c is a characteristic velocity, and A, B and are the model parameters whose relative size defines velocity strengthening or weakening behaviour. Dieterich (1978) and Ruina (1983), who added a second state variable, predict the observed exponential dependence of healing (related to hold time between sliding increments) on the peak shear stress.

Predictions outside the laboratory values are strongly dependent on the precise mathematical form of the crack velocity on stress intensity. However, in practice it may be difficult to distinguish between the exponential and power law dependence forms, given the bandwidth of the stress intensity data imposed by the minimum strain rates achievable in the laboratory (Atkinson & Meredith 1987). A similar observation holds for the strain rate dependence of differential stress in frictional slide-hold tests (Ruina 1983, Fig. 6), or in triaxial deformation tests (Costin 1987, Fig. 5.15; Lockner 1998, Fig. 8). The resolution of this question may therefore require an extrapolation of scale, stress and strain rate outside the constraints of laboratory conditions, for example an examination of deformation and failure in induced seismicity associated with mining or hydrocarbon production.

In theory, we might expect an exponential law to be better suited to the early stages of damage. In this phase, crack growth occurs independently of neighbouring cracks, and is hence likely to be reaction-limited. In constrast, a power-law form may better describe the stage where cracks grow by coalescence, for example the simple percolation model suggested by Main (1999). One of the main practical consequences of the model presented here is that power-law steady-state creep is an emergent property of the model, rather than a constraint, as in Lockner (1998).

CONCLUSIONS

A simple hybrid model for creep in the brittle field, involving the linear superposition of stable (transient) and unstable (accelerating) processes, spontaneously produces an apparent intermediary phase of 'steady-state' (secondary) creep. The model is based on the constitutive equations for time-dependent crack growth, accounting for the presence of local negative feedback or stress shielding at the crack tip, due to local hardening mechanisms, or the influence of other cracks in the population. The resulting solution is consistent with Voight's proposed form for time-dependent strain. The model exactly predicts the modified form of Omori's law for aftershock and foreshock sequences, the latter requiring a small correction for finite rupture velocity at the time of the main shock. The model also predicts the observed form of power-law creep in the apparent 'steady-state' phase. There is therefore no need to invoke three separate mechanisms (and an extra three parameters) to explain the data. The same model can be modified for the case of dynamic loading, and correctly predicts the variation of breaking stress with stress (or strain) rate, including the threshold effect observed at very small strain rates.

ACKNOWLEDGMENTS

This paper was developed and written during a sabbatical visit to the Dipartimento di Fisica at the University of Bologna. I am grateful to the staff and students there, and in particular to Francesco Mulargia, for making my stay enjoyable and productive. David Lockner and Martin Casey provided constructive and detailed reviews which improved the context, presentation, and discussion of the results.

REFERENCES

Ashby, M.F. & Hallam, S.D., 1986. The failure of brittle solids containing small cracks under compressive stress states, *Acta Metall.,* **34,** 497–510.

Ashby, M.F. & Sammis, C.G., 1990. The damage mechanics of brittle solids in compression, *Pure appl. Geophys.,* **133,** 489–521.

Atkinson, B.K. & Meredith, P.G., 1987. The theory of subcritical crack growth with applications to minerals and rocks, in *Fracture Mechanics of Rock,* pp. 111–166, ed. Atkinson, B.K., Academic Press, London.

Bufe, C.G. & Varnes, D.J., 1993. Predictive modeling of the seismic cycle of the greater San Francisco Bay region, *J. geophys. Res.,* **98,** 9871–9883.

Costin, L.S., 1987. Time-dependent deformation and failure, in *Fracture Mechanics of Rock,* pp. 167–215, ed. Atkinson, B.K., Academic Press, London.

Das, S. & Scholz, C.H., 1981. Theory of time-dependent rupture in the Earth, *J. geophys. Res.,* **86,** 6039–6051.

Davy, P., Hansen, A., Bonnet, E. & Zhang, S.-Z., 1995. Localization and fault growth in layered brittle-ductile systems: implications for deformations of the continental lithosphere, *J. geophys. Res.,* **100,** 6281–6294.

Dieterich, J.H., 1978. Time-dependent friction and the mechanics of stick-slip, *Pure appl. Geophys.,* **116,** 790–806.

Hainzl, S., Zoeller, G. & Kurths, J., 1999. Similar power laws for foreshock and aftershock sequences in a spring-block model for earthquakes, *J. geophys. Res.,* **104,** 7243–7253.

Hobbs, B.E., Means, W.D. & Williams, P.F., 1976. *An Outline of Structural Geology,* Wiley, New York.

Horii, H. & Nemat-Nasser, S., 1985. Compression-induced microcrack growth in brittle solids: axial splitting and shear failure, *J. geophys. Res.,* **90,** 3105–3125.

Kagan, Y.Y. & Knopoff, L., 1978. Statistical study of the occurrence of shallow earthquakes, *Geophys. J. R. astr. Soc.,* **55,** 67–86.

Kostrov, 1974. Seismic moment and the energy of earthquakes and seismic flow of rock, *Izv. Acad. Sci., USSR Phys. Solid Earth,* **1,** 23–44.

Lankford, J., 1981. The role of tensile microfracture in the strain rate dependence of compressive strength of fine-grained limestone, *Int. J. Rock Mech. Min. Sci. Geomech. Abstract.,* **18,** 173–175.

Lawn, B., 1993. *Fracture of Brittle Solids,* 2nd edn, Cambridge University Press, Cambridge.

Liakopoulou-Morris, F., Main, I.G., Crawford, B.R. & Smart, B.G.D., 1994. Microseismic properties of a homogeneous sandstone during fault development and frictional sliding, *Geophys. J. Int.,* **119,** 219–230.

Lockner, D., 1993a. Room temperature creep in saturated granite, *J. geophys. Res.,* **98,** 475–487.

Lockner, D., 1993b. The role of acoustic emission in the study of rock fracture, *Int. J. Rock Mech. Min. Sci. Geomech. Abstract.,* **30,** 883–899.

Lockner, D.A., 1998. A generalised law for brittle deformation of Westerley Granite, *J. geophys. Res.,* **103,** 5107–5123.

Main, I., 1988. Prediction of failure times in the earth for a time-varying stress, *Geophys. J.,* **92,** 455–464.

Main, I.G., 1999. Applicability of time-to-failure analysis to accelerated strain before earthquakes and volcanic eruptions, *Geophys. J. Int.,* **139,** F1–F6.

Main, I.G., Leonard, T., Papasouliotis, O., Hatton, C.G. & Meredith, P.G., 1999. One slope or two?—Detecting statistically-significant breaks of slope in geophysical data, with application to fracture scaling relationships, *Geophys. Res. Lett.,* **26,** 2801–2804.

Meredith, P.G. & Atkinson, B.K., 1983. Stress corrosion and acoustic emission during tensile crack propagation in Whin Sill Dolerite and other basic rocks, *Geophys. J. R. astr. Soc.,* **75,** 1–21.

Moore, D.E. & Lockner, D.A., 1995. The role of microcracking in shear-fracture propagation in granite, *J. struct. Geol.,* **17,** 95–114.

Ngwenya, B.T., Elphick, S.C., Maillot, B., Main, I.G. & Shimmield, G.B., 1999. Fluid–rock interactions during room temperature creep of porous sandstones: Implications for fault sealing, *J. geophys. Res.,* submitted.

Okui, Y. & Horii, H., 1997. Stress and time-dependent failure of brittle rocks under compression: a theoretical prediction, *J. geophys. Res.,* **102,** 14 869–14 881.

Ranalli, G., 1995. *Rheology of the Earth,* 2nd edn, Chapman & Hall, London.

Reasenberg, P.A., 1999. Foreshock occurrence before large earthquakes, *J. geophys. Res.,* **104,** 4755–4768.

Reches, Z. & Lockner, D.A., 1994. Nucleation and growth of faults in brittle rocks, *J. geophys. Res.,* **99,** 18 159–18 173.

Renshaw, C.E. & Park, J.C., 1997. Effect of mechanical interactions on the scaling of fracture length and aperture, *Nature,* **386,** 482–484.

Rice, J.R., 1978. Thermodynamics of quasi-static growth of Griffith cracks, *J. Mech. Phys. Solids,* **26,** 61–78.

Ruina, A.L., 1983. Slip instability and state variable friction laws, *J. geophys. Res.,* **88,** 359–370.

Sammis, C.G. & Ashby, M.F., 1986. The failure of brittle porous solids under compressive stress states, *Acta Metall.,* **34,** 511–526.

Sano, O., Ito, I. & Terada, M., 1981. Influence of strain rate on dilatancy and shear strength of Oshima granite under uniaxial compression, *J. geophys. Res.,* **86,** 9299–9311.

Scholz, C.H., 1968a. Microfracturing and the inelastic deformation of rock in compression, *J. geophys. Res.,* **73,** 1471–1432.

Scholz, C.H., 1968b. Microfractures, aftershocks and seismicity, *Bull. seism. Soc. Am.,* **58,** 1117–1130.

Stanley, H.E., 1971. *Introduction to Phase Transitions and Critical Phenomena,* Oxford Science, Oxford.

Utsu, T., Ogata, Y. & Matsu'ura, R.S., 1995. The centenary of the Omori formula for the decay of aftershock activity, *J. Phys. Earth,* **43,** 1–33.

Varnes, D.J., 1983. Time-dependent deformations in creep to failure of earth materials, in *Proc. 7th East Asian Geotechnical Conf.,* **2,** 107–130, Southeast Asian Geotechnical Society, Bangkok.

Voight, B., 1988. A method for predicting volcanic eruptions, *Nature,* **332,** 125–130.

Voight, B., 1989. A relation to describe rate-dependent material failure, *Science,* **243,** 200–203.